

PAPER • OPEN ACCESS

Admittance spectroscopy of InGaAsN based solar cells

To cite this article: A I Baranov *et al* 2017 *J. Phys.: Conf. Ser.* **917** 052033

View the [article online](#) for updates and enhancements.

Related content

- [Admittance Spectroscopy of ZnO Crystals](#)
Yasuo Kanai
- [Admittance Spectroscopy of ZnO Crystals Containing Ag](#)
Yasuo Kanai
- [Strain-Compensated GaAsN/InGaAs Superlattice Structure Solar Cells](#)
Pei-Hsuan Wu, Yan-Kuin Su, I-Liang Chen et al.

Admittance spectroscopy of InGaAsN based solar cells

A I Baranov^{1,2,a}, A S Gudovskikh^{1,3}, D A Kudryashov¹, A M Mozharov¹, K S Zelentsov¹, J-P Kleider²

¹ St Petersburg Academic University of RAS, 194021 St Petersburg, Russia.

² GeePs (Group of electrical engineering – Paris), UMR CNRS 8507, CentraleSupélec, Univ. Paris-Sud, Université Paris-Saclay, Sorbonne Universités, UPMC Univ Paris 06, 91192 Gif-sur-Yvette CEDEX, France.

³ St Petersburg Electrotechnical University "LETI", 197376 St Petersburg, Russia.

^abaranov_art@spbau.ru

Abstract. Single-junction InGaAs solar cells were grown by MBE with active layers based on a GaAsN/InAs superlattice. Dependence of defect formation on thickness of InGaAs was explored in the study. Thickness increase from 900 nm to 1200 nm leads to defect formation with two activation energies of 0.20 eV and 0.50 eV but the value of quantum efficiency stays almost the same. Further thickness increase up to 1600 nm leads to the increase of defect concentration in the InGaAs active layer. These defects are non-radiative recombination centres because a significant decrease of solar cell quantum efficiency was observed. The existence of a critical thickness for defect-free growth of InGaAs based on GaAsN/InAs superlattice is proposed.

1. Introduction

In 2015 multi-junction solar cells (MJ SC) based on III-V compounds with a record efficiency of 46% were fabricated [1]. Triple-junction SC based on the GaInP (1.85 eV) / GaAs (1.42 eV) / Ge (0.7 eV) system are used in industry for space applications where the key factors are efficiency and resistance to radiation. But its concentrator efficiency has almost reached the theoretical limit (46%) and now its value is more than 40% [2]. Fortunately, according to theoretical estimations an additional subcell with energy bandgap of 1 eV could increase the SC efficiency up to 52% [3]. However, such subcell should be lattice-matched to Ge and GaAs wafers. $\text{Ga}_{1-x}\text{In}_x\text{N}_y\text{As}_{1-y}$ with a small content of nitrogen is one of the most promising alloys to reach this goal. Such III-V-N alloys (GaPNAs, InGaAs etc.) with nitrogen content less than 5% are called dilute nitrides. It has been shown that the small addition of nitrogen leads to large bowing parameters for the bandgap in quaternary $\text{Ga}_{1-x}\text{In}_x\text{N}_y\text{As}_{1-y}$ alloys: already few percent of nitrogen reduces the bandgap by hundreds of meV [4] and a value of 1 eV can be achieved. Furthermore, these layers can be epitaxially grown on Ge and GaAs wafers when $y=0.35x$. Various groups [3, 5-8] studied InGaAs layers grown by epitaxy, but the quality is not sufficient for fabrication of high-efficiency solar cells. The low lifetime of charge carriers is the most crucial issue in dilute nitrides. The main reason is the high concentration of non-radiative recombination centers in active layers. In MOCVD (metal-organic chemical-vapor deposition) it comes from the background doping of carbon and hydrogen during the process. On the other hand, MBE (molecular-beam epitaxy) allows one to avoid these problems and enables to control the flow of nitrogen more precisely. However, a lower process



temperature is required for the growth of GaAsN compared with that of GaAs in MBE: it leads to defect formation reducing dramatically the lifetime in InGaNaS. Some researchers try to avoid the defect formation by addition of antimony in active layers of InGaNaSb [6]. Unfortunately, Sb can deposit on the wall of the chamber which leads to negative background doping in subsequent layers. Consequently it is necessary to have two chambers for the growth of MJ SC, but this renders the technology much more complicated.

Recently, a new method was explored for the fabrication of InGaNaS based compounds without antimony [8]. It is based on the growth of a GaAsN/InAs superlattice by MBE. In this paper properties of i- GaAsN/InAs layers in single-junction SC by admittance spectroscopy will be explored.

2. Experiments and samples

Three p-i-n structures with different thickness (900 nm, 1200 nm, 1600 nm) of active InGaNaS i-layer based on GaAsN/InAs superlattice were grown on n-type GaAs wafers by MBE using a Veeco GEN III setup with a plasma nitrogen source. A p-type GaAs layer was grown on the top as a wide-bandgap window (concentration of acceptors is 10^{19} cm^{-3}). Silicon and beryllium were used for n- and p- type doping in GaAs layers, respectively. The bandgap energy of the InGaNaS layer is equal to 1 eV as confirmed by PL measurements. Metallic Au/Ge and Au/Zn alloys were evaporated on the bottom and top side of structure, respectively, for the fabrication of contacts. Ohmic behaviour was obtained after rapid thermal annealing at 400 °C. Au/Zn was evaporated as circular contacts with diameters of 0.25, 0.5, 1 and 2 mm for capacitance measurements. Then samples were etched in a solution of $\text{H}_2\text{SO}_4:\text{H}_2\text{O}_2:\text{H}_2\text{O}=5:1:1$ for the fabrication of mesa-structures. The sample structure is schematically presented in Figure 1.

The admittance spectroscopy technique allows one to estimate the activation energy (E_a) and the capture cross section (σ_a) of the defect level from the analysis of the temperature and frequency dependence of the capacitance, $C(T,f)$, and of the conductance, $G(T,f)$ [9]. The measurements were performed using a liquid nitrogen cryostat in the temperature range from 80 K to 360 K and at frequencies from 20 Hz to 1 MHz. Three different value of bias voltage were used (-0.4 V, -0.2 V, 0.0 V) and the test signal amplitude was set to 50 mV.

| |
|--|
| Au/Zn |
| p-GaAs 200nm $1 \cdot 10^{19} \text{ cm}^{-3}$ |
| i-InGaNaS |
| n-GaAs 200nm $3 \cdot 10^{18} \text{ cm}^{-3}$ |
| n-GaAs wafer |
| Au/Ge |

Figure 1. Schematic view of the p-i-n structure with i- InGaNaS layer.

3. Results

The measured temperature and frequency dependences of the capacitance are shown in Figure 2 for zero bias voltage. The capacitance of the sample with the 900 nm thick InGaNaS layer decreases monotonously with the increase of frequency for all temperatures. No step is observed in $C(f)$ curves meaning no response from defect level in this temperature range. However, the shape of $C(f)$ curves is dramatically changed when the InGaNaS layer thickness is increased to 1200 nm. Detailed analysis of $C(f)$ curves allows one to observe two small steps: a first step at low temperatures 100..220 K and a

second step at high temperatures 320..360 K. These steps can be caused either by bulk defect levels in the undoped layer or by interface states at InGaNaS/GaAs heterojunctions. The step position in $C(f, T)$ curves does not depend on applied bias voltage (measurements are not shown here) indicating that the response originates from bulk defects rather than from the InGaNaS/GaAs interface. Further increase of thickness to 1600 nm leads to a drastic increase of the amplitude of the first step while the second step in $C(f)$ curves remains the same (Figure 2c).

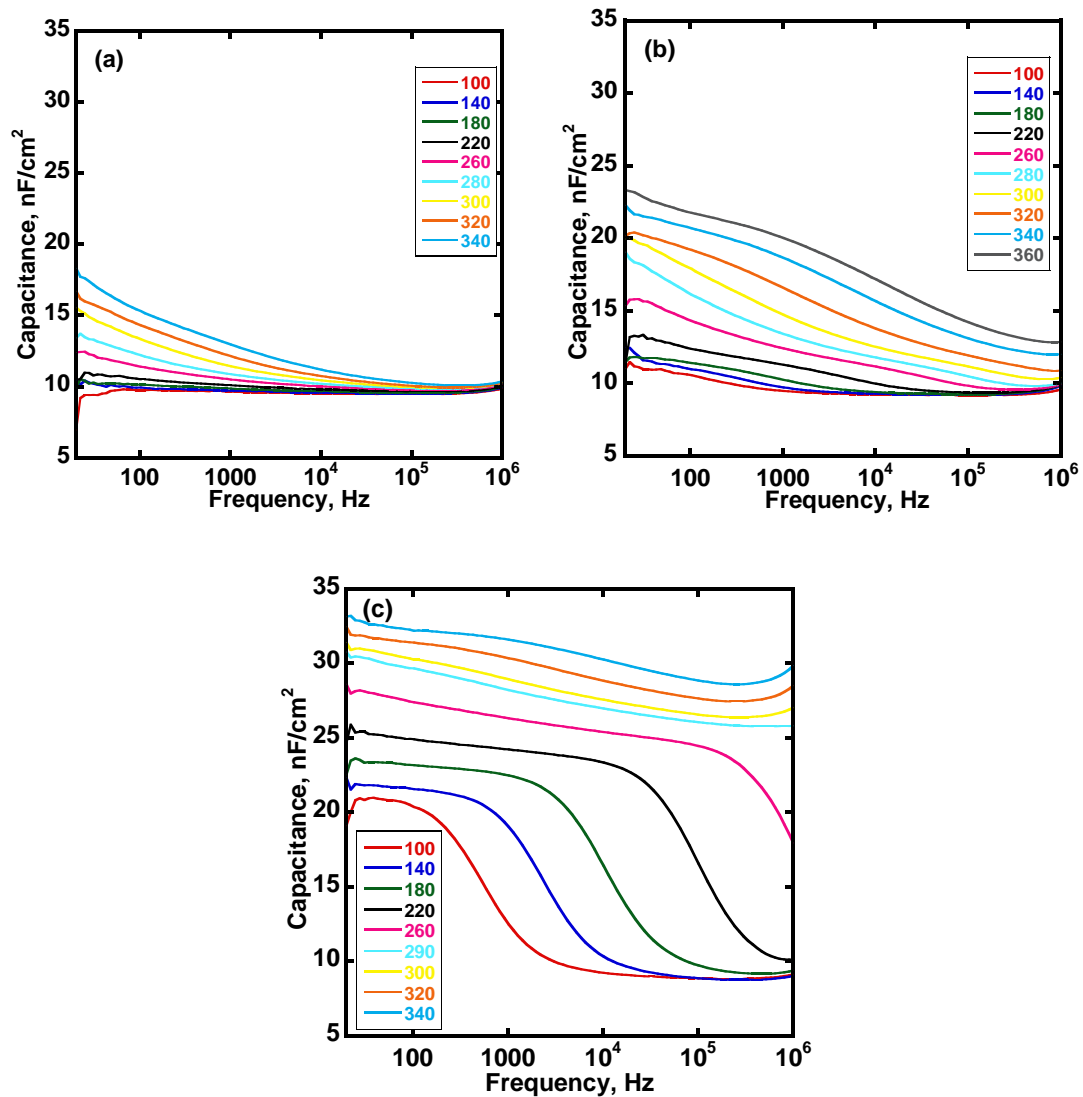


Figure 2 (a, b, c). $C(T, f)$ curves for SC with InGaNaS active layers with thickness of: 900 nm (a), 1200 nm (b), and 1600 nm (c).

Arrhenius plots of f/T^2 (f and T being the turn-on frequency and temperature, respectively, of the capacitance step, or of the maximum of the related conductance peak) are used to derive the activation energy and capture cross section (from the extrapolation to infinite temperature) of the defect responsible for the capacitance step. The Arrhenius plots are shown in Figure 3 for both structures with i-InGaNaS thickness of 1200 nm and 1600 nm. For the sample with i-layer thickness of 1200 nm the low-temperature defect level has an activation energy (E_a) of 0.20 eV and a capture cross section (σ) of $7.2 \times 10^{-17} \text{ cm}^2$ while the high-temperature defect has parameters $E_a = 0.46 \text{ eV}$ and $\sigma = 6.3 \times 10^{-16} \text{ cm}^2$,

respectively. For the sample with 1600 nm thick i-layer the low-temperature defect level has parameters $E_a = 0.18$ eV and $\sigma = 6.4 \times 10^{-17} \text{cm}^2$ and for the high-temperature $E_a = 0.54$ eV and $\sigma = 1.5 \times 10^{-14} \text{cm}^2$. Taking into account the uncertainty in the experimental measurements we can conclude that the parameters of the both high-temperature and low-temperature levels are similar in both samples, meaning that it is a characteristic feature of the i-InGaNaS layer based on the GaAsN/InAs superlattice.

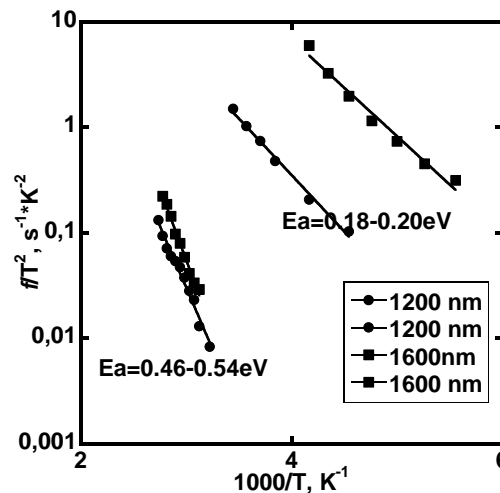


Figure 3. Arrhenius plot of f/T^2 for the two steps detected in the 1200 nm and 1600 nm thick i-InGaNaS samples.

Parameters of the high-temperature defect detected in our i-InGaNaS layers correspond to previously described defects with an activation energy of 0.50 eV in literature [7, 10]. Such defects located in the middle of the InGaNaS bandgap (1 eV) can be considered as centers of strong non-radiative recombination leading to low charge carriers lifetime in these active layers. In our previous study [8] we showed the dependence of external quantum efficiency on thickness for these samples (Figure 4). From experimental results of admittance spectroscopy and quantum efficiency we can conclude that, when the thickness increases from 900 nm to 1200 nm conditions become more favorable for the formation of defects in InGaNaS. But their concentration is too low to affect the quantum efficiency of SC. Quantum efficiency decreases slightly in the short wavelength range due to recombination losses while it slightly increases in long wavelength range because of enhanced absorption with the thickness increase. Further thickness increase to 1600 nm leads to significant increase of defect concentration in active layers and extremal decrease of quantum efficiency of SC. Obviously, the detected defects can be centers of non-radiative recombination which lead to degradation of photoelectrical properties of InGaNaS. Unfortunately, admittance spectroscopy does not allow one to estimate the absolute value of defect concentration directly, but future experiments will be based on deep-level transient spectroscopy (DLTS) technique for a more precise determination of detected defects parameters.

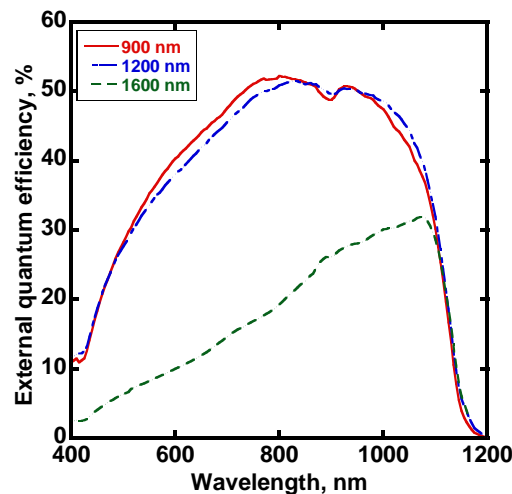


Figure 4. External quantum efficiency of p-i-n structures with i- InGaAs layers.

4. Conclusion

The dependence of defect formation on the thickness of the i- InGaAs layer based on GaAsN/InAs superlattices was explored in this study. Increase of thickness from 900 nm to 1200 nm leads to the start of defect formation with two activation energies of 0.20 eV and 0.50 eV but the quantum efficiency does not change significantly. Further thickness increase up to 1600 nm leads to high defect concentrations in the InGaAs active layers and to a significant decrease of quantum efficiency of solar cells. The existence of a critical thickness for defect-free growth of InGaAs based on GaAsN/InAs superlattices can thus be emphasized.

Acknowledgements

The reported study was funded by RFBR in the framework of the research project No. 16-38-00791.

References

- [1] Green M A, Emery K, Hishikawa Y et al. 2015 Prog. Photovolt. Res. Appl. **23** 1
- [2] King R R, Law D C, Edmondson K M et al. 2007 Appl. Phys. Lett. **90** 183 516
- [3] Yamaguchi M, Nishimura K I et al. 2008 Solar Energy **82** (2), 173
- [4] Weyers M, Sato M, Ando H 1992 Jpn. J. Appl. Phys. **31** (2) 7A, L853
- [5] Tzung-Han Wu et al. 2011 Jpn. J. Appl. Phys. **50** 01AD07
- [6] Jackrel D B, Bank S R et al. 2007 J. Appl. Phys. **101** 114916
- [7] Polojärvi V, Aho A et al. 2016 Sol. Ener. Mat. & Sol. Cells **149** 213
- [8] Nikitina E V, Gudovskikh A S et al. 2016 Semiconductors **50** (5) 663
- [9] Losee D L 1975 J. Appl. Phys. **46**(5) 2204
- [10] Johnston S, Ahrenkiel R, Ptak A et al. 2003 No. NREL/CP-520- 33557, National Renewable Energy Laboratory (NREL), Golden, Colorado, USA